

Topology Characterization of High Density Airspace Aeronautical Ad Hoc Networks *

Daniel Medina, Felix Hoffmann, Serkan Ayaz
Institute of Communications and Navigation
German Aerospace Center (DLR)
Munich, Germany
Daniel.Medina@dlr.de

Carl-Herbert Rokitansky
Department of Computer Science
University of Salzburg
Salzburg, Austria
roki@cosy.sbg.ac.at

Abstract

Aeronautical ad hoc networks represent a special type of ad hoc wireless networks, given their significantly larger scale and the distinct characteristics of their mobile nodes. Aircraft populate the international airspace very heterogeneously. Some regions experience highly dense air traffic, with aircraft headings being largely uncorrelated. Other regions remain only very sparsely populated, with aircraft typically flying parallel to each other. Moreover, the number of airborne aircraft in a given region changes significantly throughout the day. In this paper, we focus on the densely populated European airspace, and investigate the topological behavior of multihop ad hoc wireless networks formed by air-air links of varying communications range. We derive analytical expressions for various topological aspects, such as the lifetime of inter-aircraft links, and the projected hop length using greedy forwarding. These results are in good agreement with the behavior observed in our simulations of the European air traffic scenario. In addition, we assess the performance of greedy forwarding in the aeronautical environment and show that, under moderate connectivity, this technique delivers almost all packets to their destinations with a minimum hop count.

1. Introduction

Multihop air-air communications represent an attractive alternative to satellite-based communications for aviation in areas where aircraft have no direct air-ground radio coverage. Benefits include lower latency, ease of deployment and higher data rates per unit cost.

In [2], we demonstrated the topological feasibility of an aeronautical ad hoc network over the North Atlantic Cor-

ridor, based on realistic air traffic patterns and taking into account the long range of air-air links. In this oceanic environment, aircraft density is relatively low, resulting in a sparse network topology. In addition, nodes move in virtually the same direction (either eastward or westward), giving rise to a very stable topology.

In this paper, we investigate the topological properties of aeronautical ad hoc networks in a radically different scenario, where the node spatial density is significantly higher and nodes move at random angles to each other: the European airspace. As in [2], we propose the use of position-based greedy forwarding and use simulations to assess the performance of this attractive routing technique, considering various performance metrics such as packet delivery ratio and average number of hops.

Our simulations are based on the airline flight schedule database published by IATA [3], containing among other information the departure and destination airports and schedules of all aircraft in operation today. Flight trajectories have been idealized by interpolating between departure and destination airports with great circle arcs, corresponding to the shortest distance between two points on the surface of the earth.

The remainder of this paper is organized as follows. Section 2 briefly summarizes related work in the relatively new field of aeronautical ad hoc networks. Our network model is described in Section 3. In Section 4, we investigate the network connectivity for various air-air transmission ranges. In Section 5, we derive an analytical expression for the inter-aircraft link lifetime. The applicability of greedy forwarding to the aeronautical environment is investigated in Section 6, where we perform a stochastic analysis of the hop length and compare it with our simulation results. Finally, Section 7 summarizes our main conclusions, provides an outlook for future research and concludes the paper.

*This work is partially funded by the European Commission through the NEWSKY project [1] under contract no. 37160.

2. Related Work

Some attention has recently been drawn to the application of ad hoc wireless networking to the aeronautical environment [4] [5] [6].

The AeroSat Corporation [7], founder of the Airborne Internet Consortium (AIC) [8], has performed flight trials with directional Ku-band antennas, demonstrating air-air links of up to 45 Mbps at ranges of up to 300 nautical miles [9].

This paper studies the applicability to aeronautics of existing ad hoc network concepts, on which recent research work exists. Gateway discovery and selection strategies in ad hoc networks have recently been subject to study within the AUTOCONF WG in IETF [10][11]. Recent proposals for the integration of IP mobility and mobile ad hoc networks can be found in [12]. Geographic ad hoc routing has been studied e.g. in [13][14]. Recent papers have investigated the performance of this technique in vehicular environments [15][16], with very promising results.

3. Network Model

Our aeronautical ad hoc network is composed of two types of nodes: aircraft and ground stations. While in range of a ground station, aircraft access ground services via a direct air-ground (A/G) link. Otherwise, the aircraft make use, whenever possible, of an air-air (A/A) multihop path to a ground station. Ground stations are equipped to serve as gateways for the aeronautical ad hoc network. In the following, we refer to ground stations as Internet Gateways (IGWs), following current IETF practice.

Our area of interest, shown in Fig. 1, corresponds to the geographic region between 35°N, 60°N, 10°W and 30°E. We have placed five IGWs within this area, each at a major European airport (London, Paris, Frankfurt, Munich, Madrid).¹ Fig. 2 shows a snapshot of the air traffic situation in this region around 5:00 GMT on an average day.

3.1. Gateway discovery and selection

IGWs periodically flood IGW advertisements (IGWADV)s over the airborne ad hoc network to let aircraft know of their existence. These advertisements contain an IP address prefix owned by the IGW, from which the aircraft can configure a care-of address, and a Hop Count field, which is set to one by the ground station and incremented by each forwarding aircraft. Aircraft periodically receive IGWADV)s from potentially multiple IGWs, and populate their Reachable Ground Station Set (RGSS) table accordingly. Each RGSS entry contains the IGW identifier, the

¹This representative set of major European airports has been chosen as an example of a possible initial deployment.



Figure 1. Area of interest showing the placement of ground stations.

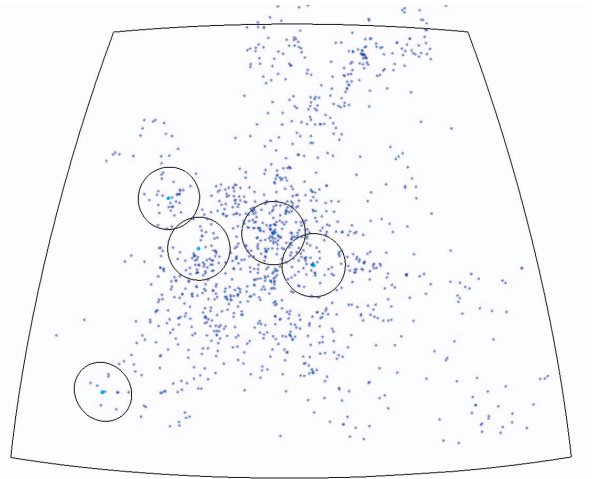


Figure 2. Snapshot showing the aircraft distribution in European airspace around 5:00 GMT.

advertised prefix, and the current minimum hop distance to the IGW, extracted from the Hop Count field. The gateway selection mechanism is based on hop distance, that is, each aircraft selects the topologically closest IGW as the destination for its own traffic, and configures its care-of address from this IGW. Similarly, each IGW maintains a table of aircraft that have configured a care-of address from it, and forwards internet traffic to those aircraft. We define the IGWADV interval α as the time elapsed between two consecutive IGWADV)s sent by an IGW, and assume it to be the same for all IGWs. Each RGSS entry includes a lifetime field. If the lifetime for an entry expires, the entry is

removed from the RGSS.

3.2. Greedy Forwarding

Routing in the ad hoc network is based on *greedy forwarding*. In this technique, packets are marked by their originator with their destination's location. As a result, a forwarding node can make a locally optimal, greedy choice in choosing a packet's next hop. Specifically, if a node knows its radio neighbors' positions, the locally optimal choice of next hop is the neighbor geographically closest to the packet's destination. Mathematically, node i forwards a packet meant for destination node j to node n such that

$$d_{nj} = \min_k d_{kj}, \quad k \in \{\mathcal{N}_i \cup i\} \quad (1)$$

where \mathcal{N}_i represents the set of neighbors of node i and d_{kj} denotes the great circle angular distance (in radians) between neighbor k and destination node j , given by

$$d_{kj} = \cos^{-1} \left(\sin \theta_k \sin \theta_j + \cos \theta_k \cos \theta_j \cos(\phi_k - \phi_j) \right) \quad (2)$$

where (θ_k, ϕ_k) denote the latitude and longitude of node k , respectively. Forwarding in this regime follows successively closer geographic hops, until the destination is reached.

If node i has no neighbors geographically closer to the destination than itself, we have $n = i$, and the packet is dropped. In this case, node i is said to be a *local maximum*. A number of solutions have been proposed to circumvent this problem [13]. However, for the sake of simplicity, we consider pure greedy forwarding in our simulations.

Civil aviation aircraft have the advantage of knowing their precise position at all times via e.g. a Global Navigation Satellite System (GNSS), such as GPS. In addition, these aircraft are expected to use Automatic Dependent Surveillance - Broadcast (ADS-B) in the near future to periodically beacon their state vector to surrounding aircraft, including their position and velocity vector. This means every aircraft is aware of its own position and all of its neighbors' positions at all times.

However, there is still a need for the aircraft to determine the position of the destination IGW, and for the IGW to determine the position of the aircraft:

a) For the former case, we include the position information of the IGW in the IGWADV. Alternatively, aircraft could cache a table of all operational IGWs and their positions while at the gate. This would reduce the overhead by keeping IGWADV smaller (since they would not carry the IGW position). This table would be looked up when an aircraft needs to send a packet to a certain IGW, to determine the IGW position.

b) For the latter case, since the position of the aircraft changes over time, the aircraft must periodically unicast Position Updates (PUs) back to its selected IGW, containing its current position and possibly a time stamp. When a packet needs to be sent to the aircraft, the IGW uses the last two PUs to estimate the current position of the aircraft. We define the PU interval T as the time elapsed between two consecutive PUs. The current position estimate is computed assuming great circle trajectories as follows. If the last two PUs are given by

$$\mathcal{P}_{n-1} \equiv (\theta_{n-1}, \phi_{n-1}) @ t_{n-1}$$

$$\mathcal{P}_n \equiv (\theta_n, \phi_n) @ t_n$$

with $T = t_n - t_{n-1}$, the aircraft's true course $\psi_n \in [-\pi, \pi]$ is given by

$$\psi_n = \pm \cos^{-1} \frac{\sin \theta_n - \sin \theta_{n-1} \cos d_{n,n-1}}{\cos \theta_{n-1} \sin d_{n,n-1}} \quad (3)$$

where the negative sign applies if $\sin(\phi_n - \phi_{n-1}) < 0$, and $d_{n,n-1}$ is computed as in (2). The angular distance covered by the aircraft at time t from $(\theta_{n-1}, \phi_{n-1})$ is given by

$$d(t) = \frac{t - t_{n-1}}{T} d_{n,n-1}. \quad (4)$$

The position of the aircraft at time t can then be computed as

$$\theta(t) = \sin^{-1} \left(\sin \theta_{n-1} \cos d(t) + \cos \theta_{n-1} \sin d(t) \cos \psi_n \right)$$

$$\phi(t) = \left(\phi_{n-1} + \sin^{-1} \frac{\sin \psi_n \sin d(t)}{\cos \theta(t)} + \pi \right) \bmod 2\pi - \pi$$

for $t_n < t < t_n + T$.

Position updates need not be very frequent, since aircraft headings rarely change. Since PUs are unicast back to the IGW and not flooded over the network, overhead is not a big concern. They could also be piggybacked onto payload packets. Alternatively, if the ground station operator receives up-to-date position information about all aircraft directly from the relevant aircraft operator through the ground network, these PUs would not be needed.

3.3. Link model

Since our focus in this paper is on topological aspects, we make use of an idealized communications link model. We consider an omnidirectional transmission range, denoted by r , which is a variable in our simulations. A link exists between two nodes if the distance between them is less than r . It is worth noting that in aeronautical communications, the available transmit power is virtually unlimited (apart from technological constraints). However, the theoretical maximum transmission range between two nodes is

limited by the horizon for typical line-of-sight communications. Assuming a flight altitude of 35000 ft, an air-ground link may reach up to approx. 225 nmi (nautical miles), whereas an air-air link may reach up to approx. 450 nmi [17].

4. Connectivity

Fig. 3 shows the number of airborne aircraft found within the area of interest throughout the day.²

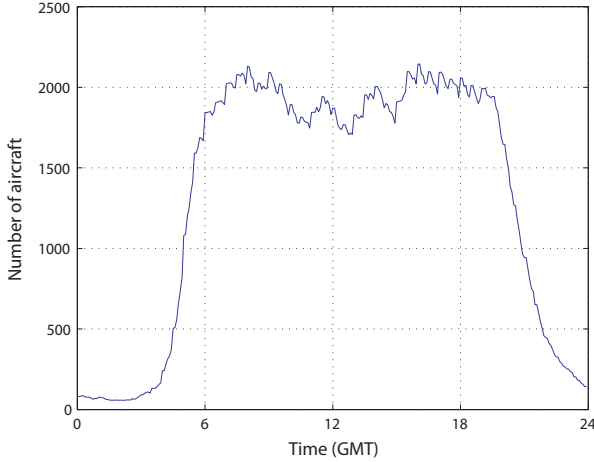


Figure 3. Variation in the number of airborne aircraft in European airspace throughout the day.

The number of airborne aircraft remains fairly stable throughout the day at around two thousand, decreasing drastically to less than a hundred aircraft at night.

We define the *connectivity* \mathcal{C} of the network as the fraction of all aircraft that have at least one multihop path to an IGW at a given time.³ We refer to such aircraft as *connected aircraft*. Mathematically,

$$\mathcal{C}(t) = \frac{\text{number of connected aircraft at time } t}{\text{total number of aircraft at time } t}.$$

Fig. 4 shows the variation in connectivity over 24 hours for several values of the air-air transmission range.

An air-air transmission range of 25 nmi is not sufficient to guarantee an acceptable level of network connectivity. On the other hand, a range of 50 nmi is sufficient to provide connectivity to almost all aircraft most of the time. Note

²This curve changes slightly from one day to another, depending on the amount of European air traffic. We have chosen a representative average day for our simulations.

³Aircraft directly connected to a ground station are not taken into account.

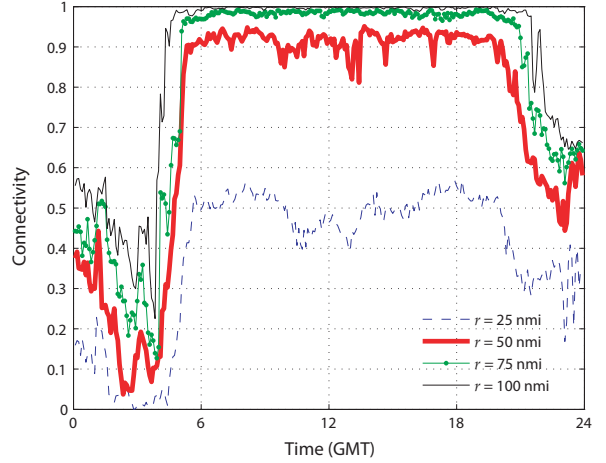


Figure 4. Variation in connectivity to the ground infrastructure throughout the day.

that even a range of 100 nmi would not be enough to guarantee connectivity at night. The number of aircraft during this period is simply too low to set up a multihop path to a ground station. However, only a few aircraft, those flying at night, are affected by this lack of connectivity.

We have also investigated ground connectivity from the perspective of a single aircraft, rather than the whole network, that is, what percentage of the flight duration the aircraft can reach the ground. We denote this quantity by μ , that is,

$$\mu = \frac{\text{total connected time}}{\text{flight duration}}.$$

Notably, many aircraft are permanently connected to the ground throughout the flight. Table 1 gives the mean value $\bar{\mu}$, averaged over all flights, for the four ranges considered. In addition, the percentage of flights for which $\mu > 0.99$ is given.

Table 1. Percentage of Aircraft with Permanent Internet Connectivity

r	25 nmi	50 nmi	75 nmi	100 nmi
$\bar{\mu}$	46%	87%	95%	98%
$\mathcal{P}(\mu > 0.99)$	21%	63%	86%	93%

Already with $r=50$ nmi, almost two thirds of the flights have virtually permanent connectivity to the ground. For this range value, an aircraft is connected to the ground on average 87% of its flight duration.

5. Inter-Aircraft Link Lifetime

To investigate the stochastic properties of the inter-aircraft link lifetime we consider two aircraft, as shown in Fig. 5. We assume linear uniform motion, i.e. each aircraft flies on a straight line *ad infinitum*, with constant speed. We further assume the aircraft course (direction of flight) is uniformly distributed in all directions.⁴ For simplicity, we let aircraft 1 fly along the positive x axis, while aircraft 2's course, denoted by θ , is chosen randomly according to the uniform distribution between 0 and 2π .

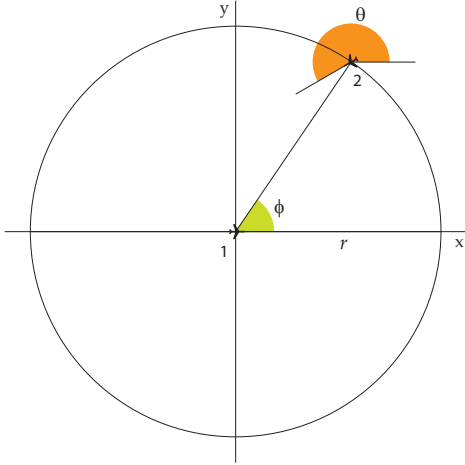


Figure 5. Setup for computation of the inter-aircraft link lifetime.

For a link between the two aircraft to occur, at some point in time aircraft 2 must traverse the coverage area of aircraft 1, determined by the air-air transmission range r (omnidirectional antennas are assumed). Assuming a uniformly distributed airborne ad hoc network, the direction from which aircraft 2 is first (or last) *seen* by aircraft 1 is itself a uniformly distributed random variable, denoted by ϕ .

The duration of a link between the two aircraft will depend on the angular separation between their directions of motion, as well as on their relative positions at the time of first (or last) contact. We define the *inter-aircraft link lifetime* $T(\theta, \phi)$ as a new random variable which is a function of the two random variables θ and ϕ .

If the situation shown in Fig. 5 corresponds to $t = 0$, the position vectors of the two aircraft are given by

$$\mathbf{r}_1(t) = v_1 t \hat{\mathbf{x}} \quad (5)$$

$$\mathbf{r}_2(t) = (r \cos \phi + v_2 t \cos \theta) \hat{\mathbf{x}} + (r \sin \phi + v_2 t \sin \theta) \hat{\mathbf{y}} \quad (6)$$

where v_1 and v_2 are the aircraft velocities and $\hat{\mathbf{x}}$ and $\hat{\mathbf{y}}$ are the axis unit vectors. The relative position vector of aircraft 2 as seen from aircraft 1 is then given by

$$\Delta \mathbf{r}(t) = (r \cos \phi + (v_2 \cos \theta - v_1)t) \hat{\mathbf{x}} + (r \sin \phi + v_2 t \sin \theta) \hat{\mathbf{y}} \quad (7)$$

By requiring that the length of this vector be equal to the transmission range r , i.e.

$$\|\Delta \mathbf{r}(t)\| = r \quad (8)$$

we can obtain the instants in time at which the aircraft experience first and last contact. These instants may in general lie in the past and/or future with respect to the instant $t = 0$. Solving (8) and subtracting the two solutions t_1 and t_2 we get

$$T(\phi, \theta) = \frac{2r|v_2 \cos(\phi - \theta) - v_1 \cos \phi|}{v_1^2 + v_2^2 - 2v_1 v_2 \cos \theta} \quad (9)$$

If $v_1 = v_2 = v$, and defining the *range-velocity ratio* $\tau = r/v$, this becomes

$$T(\phi, \theta) = \tau \left| \frac{\sin \theta}{1 - \cos \theta} \sin \phi - \cos \phi \right| \quad (10)$$

Since we know the statistical distributions of θ and ϕ (uniform), we can compute the probability density function $f_T(t)$ of random variable T , obtaining (see appendix)

$$f_T(t) = \frac{2}{\pi^2 t} \tanh^{-1} \frac{2\frac{t}{\tau}}{1 + (\frac{t}{\tau})^2} \quad (11)$$

where $0 \leq t < \infty$. This distribution is shown in Fig. 6. As indicated, 50% of the inter-aircraft links last longer than τ .

Fig. 7 shows the probability distribution of link duration collected in our simulations for $r = 100$ nmi. The peak value suggests a range-velocity ratio $\tau \approx 20$ min, corresponding to an average aircraft velocity $v \approx 600$ km/h. It is worth noting that, since we have simulated European domestic air traffic, flights are rarely longer than two or three hours. This explains the absence of long lasting links, as opposed to the theoretical asymptotic behavior shown in Fig. 6.

⁴Note that this may not hold in general in aeronautical ad hoc networks, e.g. in oceanic environments where all aircraft fly in the same direction (see [2]).

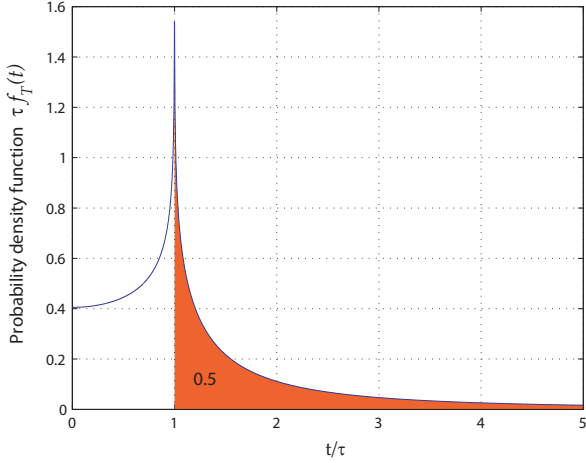


Figure 6. Probability density function $f_T(t)$ (normalized).

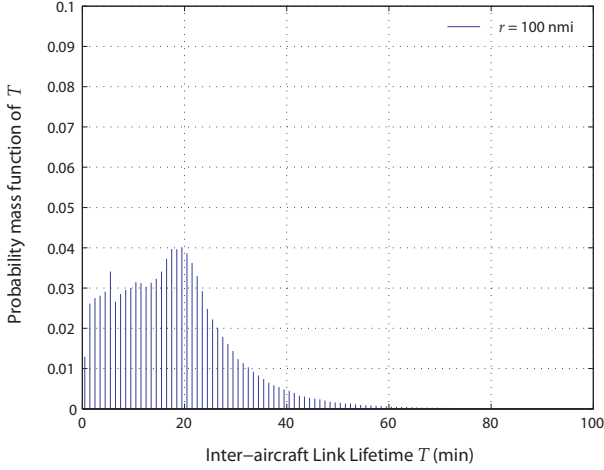


Figure 7. Simulated probability distribution of T for $r = 100$ nmi.

6. Greedy Forwarding

In this section, we analyze the relationship between the network topology and the performance of greedy forwarding, and compare our analytical derivations with simulation results.

6.1. Projected Hop Length

Greedy forwarding takes packets progressively closer to their destination, with each hop contributing to a fraction of the total distance from source node to destination node.

As illustrated in Fig. 8, we define the *projected hop length* X as the projection of the distance from the transmitting node A to the next hop B on the destination node's direction (for simplicity we choose the positive x axis). According to greedy forwarding, node B is node A 's neighbor located closest to the final destination, implying that all other neighbors would produce a smaller projection. The projected hop length is a random variable, given the random distribution of the neighbors' locations.

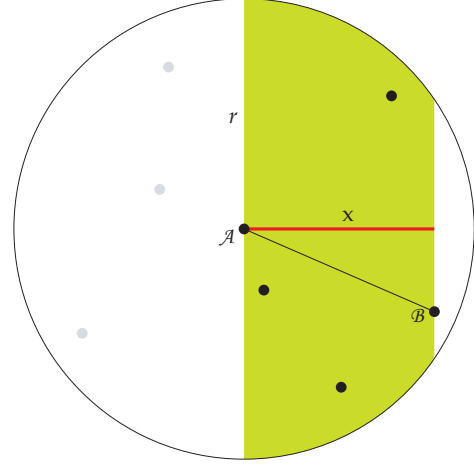


Figure 8. Definition of the projected hop length X .

Since nodes on the left semicircle do not contribute to greedy forwarding, we consider only the right semicircle, which we assume populated by n nodes. The case where none of A 's neighbors are closer to the destination than A itself (*dead end* or *local maximum*) corresponds to $n = 0$. To compute the cumulative distribution function (CDF) of X in the presence of n neighbors on the right semicircle, $F_X(x|n) = \mathcal{P}\{X \leq x | n\}$, we require that all nodes be located within the green area shown in Fig. 8. Assuming uniformly distributed node location, the probability that all nodes are in the green area is simply the n th power of the ratio between the green area and the semicircle area. This can be mathematically expressed as follows:

$$F_X(x|n) = \left(1 - \frac{2}{\pi} \left(\cos^{-1} \frac{x}{r} - \frac{x}{r} \sqrt{1 - \left(\frac{x}{r}\right)^2} \right)\right)^n, \quad x \in [0, r] \quad (12)$$

Assuming an ad hoc network with nodes randomly placed according to a two-dimensional Poisson distribution and a mean node density ζ , the probability that the right hand side semicircle has a population of n nodes is given by

$$P_n[n] = \frac{1}{n!} \left(\frac{\pi r^2}{2} \zeta\right)^n e^{-\frac{\pi r^2}{2} \zeta} \quad (13)$$

Therefore, we can obtain the unconditional CDF of X as

$$F_X(x) = \sum_{n \geq 0} P_n[n] F_X(x|n) = e^{-\frac{\pi r^2}{2} \zeta} \sum_{n \geq 0} \frac{1}{n!} \left(\frac{\pi r^2}{2} \zeta - r^2 \zeta \left(\cos^{-1} \frac{x}{r} - \frac{x}{r} \sqrt{1 - \left(\frac{x}{r}\right)^2} \right) \right)^n = e^{-r^2 \zeta \left(\cos^{-1} \frac{x}{r} - \frac{x}{r} \sqrt{1 - \left(\frac{x}{r}\right)^2} \right)}, \quad x \in [0, r] \quad (14)$$

The probability density function (PDF) can be obtained by differentiation, yielding

$$f_X(x) = e^{-\frac{\pi r^2}{2} \zeta} \delta(x) + 2r\zeta \sqrt{1 - \left(\frac{x}{r}\right)^2} e^{-r^2 \zeta \left(\cos^{-1} \frac{x}{r} - \frac{x}{r} \sqrt{1 - \left(\frac{x}{r}\right)^2} \right)} \quad (15)$$

with $x \in [0, r]$. The $\delta(x)$ component is caused by the CDF being nonzero at $x = 0$, which in turn accounts for the nonzero probability of a local maximum ($n = 0$).

Fig. 9 shows the distribution of X for $r = 1$ and different values of the node density ζ .

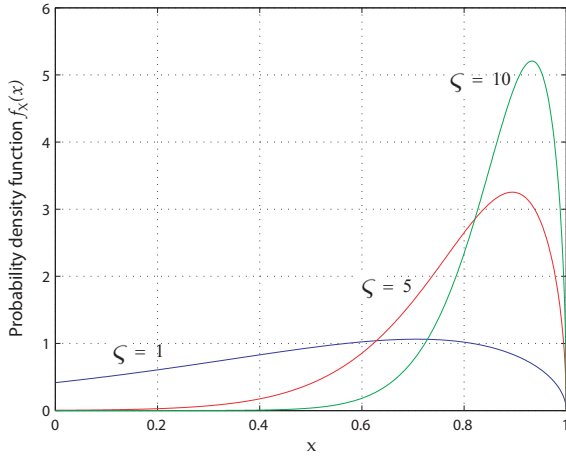


Figure 9. Probability density function $f_X(x)$ for different node density values (the $\delta(x)$ components are not shown).

Fig. 10 shows the probability distribution of X , as collected in our simulations for $r = 100$ nmi, together with the theoretical curve corresponding to an average node density $\zeta = 5 \cdot 10^{-4} \text{ km}^{-2}$. The slight discrepancy between these curves is due to the fact that the theoretical formula assumes

a uniformly distributed ad hoc network, whereas the simulated network does not truly conform to this assumption (see Fig. 2). In particular, regions where density is relatively low contribute to increase the frequency of occurrence of lower values of X .

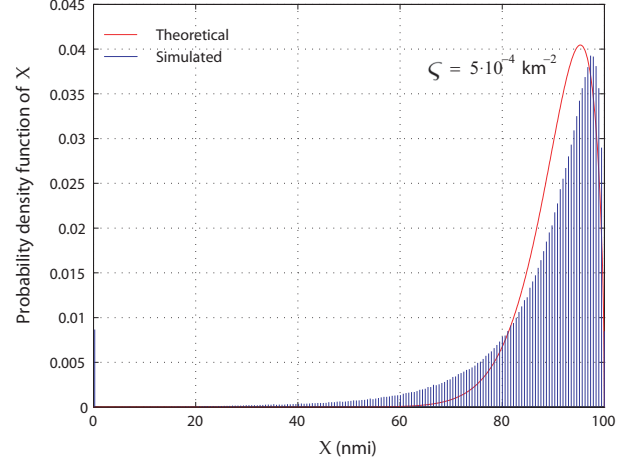


Figure 10. Simulated and theoretical probability distribution of X for $r = 100$ nmi.

6.2. Packet Delivery Ratio

The *packet delivery ratio* is defined as the percentage of transmitted packets that are successfully delivered to their destination. In our idealized network, there are only two reasons why a packet may be dropped along the multihop path from source to destination:

1. The source (aircraft or IGW) has lost topological connectivity to the destination, but is not yet aware of this, due to stale information in the RGSS or aircraft table, respectively.
2. Even though a multihop path may exist, the packet may arrive at a local maximum, and be dropped there.

In order to isolate the connectivity problem from the performance of greedy forwarding in the ad hoc network, we have initially considered an IGWADV interval $\alpha = 1s$. In this way, we avoid having stale information in the RGSS and aircraft tables. The variation in packet delivery ratio over 24 hours under these idealized conditions is shown in Fig. 11.

It is important to emphasize that by setting $\alpha = 1s$, the only remaining reason for packets to be dropped is the presence of local maxima. In other words, if there were no local maxima in the topology, all packets would be successfully delivered. Fig. 11 demonstrates the strong dependence between the frequency of occurrence of local maxima and

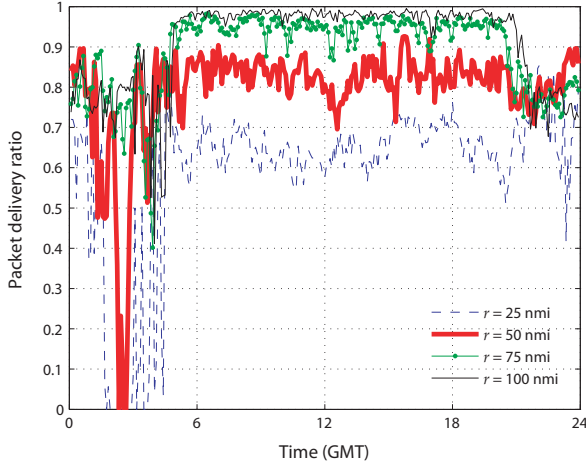


Figure 11. Variation in the packet delivery ratio throughout the day, for $\alpha = 1s$.

the air-air transmission range. With a 25 or 50 nautical mile range, the path between source and destination often encounters a local maximum, since connectivity is rather weak. This situation can be observed at several locations in the topology shown in Fig. 12.

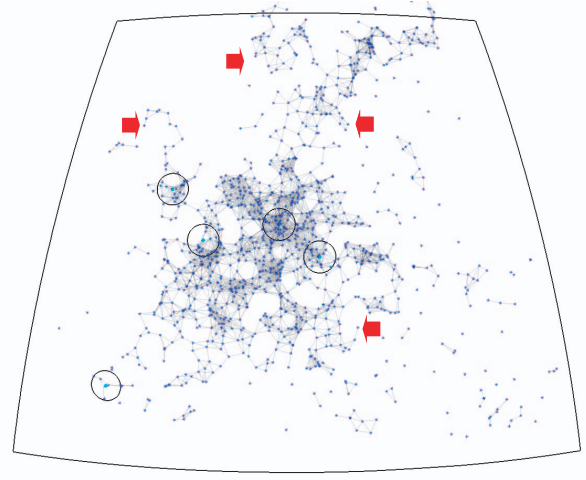


Figure 12. Example network topology showing local maxima at various locations ($r = 50$ nmi).

On the other hand, by increasing the transmission range, the richer connectivity significantly reduces the occurrence of local maxima. This can be observed in Fig. 13.

We have considered in addition the percentage of successfully delivered packets sent by a given aircraft through-

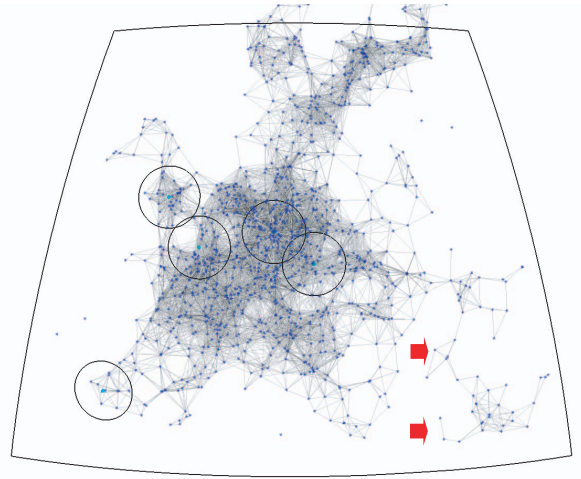


Figure 13. Example network topology showing how increasing the transmission range reduces the occurrence of local maxima ($r = 100$ nmi).

out its entire flight. We denote this quantity by η , that is,

$$\eta = \frac{\text{number of successfully delivered packets}}{\text{total number of generated packets}}.$$

Table 2 gives the mean value $\bar{\eta}$, averaged over all flights, for the four ranges considered. In addition, the percentage of flights for which $\eta > 0.99$ is given.

Table 2. Statistics of Packet Delivery Ratio

r	25 nmi	50 nmi	75 nmi	100 nmi
$\bar{\eta}$	64%	78%	94%	97%
$\mathcal{P}(\eta > 0.99)$	18%	37%	63%	74%

With $r=75$ nmi, almost two thirds of the flights have virtually all their generated packets successfully delivered to an IGW. For this range value, on average 94% of an aircraft's generated packets are successfully delivered to an IGW by greedy forwarding.

Simulations of the same scenario with an extended advertisement interval $\alpha = 600s$ have shown no significant performance degradation in terms of packet delivery ratio. Notably, the greedy forwarding technique, by not taking into account global topological information, works well even in the presence of stale information.

6.3. Average Number of Hops

As a second performance metric, we have investigated how many hops greedy forwarding requires to deliver packets to their destination, denoted by h_{GF} , in particular when compared to the topological minimum hop distance h_{SP} , as in shortest path routing. Note that we deliberately exclude paths of length 1, since these correspond to aircraft that are directly connected to a ground station.

The average number of hops obtained in our simulations with greedy forwarding \bar{h}_{GF} and shortest path routing \bar{h}_{SP} are summarized in Table 3.

Table 3. Average Number of Hops with Greedy Forwarding and Shortest Path Routing

r	25 nmi	50 nmi	75 nmi	100 nmi
\bar{h}_{SP}	5.97 hops	5.72 hops	5.02 hops	4.33 hops
\bar{h}_{GF}	6.04 hops	5.82 hops	5.09 hops	4.38 hops

Compared to the shortest path, the path chosen by greedy forwarding is on average less than 0.1 hops longer. This reveals yet another strength of the greedy forwarding technique in our airborne network, in that it very often results in packets following the shortest path (or one of the possibly multiple shortest paths), without requiring every node to have global topological information about the network.

7. Conclusion

This paper has investigated the applicability of mobile ad hoc networking concepts to aeronautical ad hoc networks formed by commercial aircraft in the European airspace environment, with a sample distribution of Internet Gateways. This scenario presents very different challenges than e.g. oceanic environments, since the node spatial density is significantly higher. By modeling the mobility of aircraft with linear uniform motion, the lifetime of inter-aircraft links has been computed in statistical terms, showing how the link and topology stability depends on the range-velocity ratio, which is relatively high in aeronautical networks, when compared to vehicular networks. In addition, the statistics of the projected hop length achieved by greedy forwarding have been derived analytically. Simulation results of the European airspace ad hoc network confirm the derived analytical expressions, even though some discrepancy exists given the non-uniform airborne aircraft distribution at any time during the day. In addition, we have assessed the performance of greedy forwarding in the aeronautical

environment and shown that, under moderate connectivity, this technique delivers almost all packets to their destinations with a minimum hop count. Further work in this area will consider issues such as power and topology control and beamforming antennas, which are expected to have significant implications on the performance of this newly emerging type of ad hoc wireless networks.

A. Derivation of $f_T(t)$

For a given ϕ , we can compute the conditional CDF of T as follows:

$$\begin{aligned}
 F_T(t|\phi) &= \mathcal{P}\{T \leq t\} \\
 &= \mathcal{P}\left\{\tau \left| \frac{\sin \theta}{1 - \cos \theta} \sin \phi - \cos \phi \right| \leq t\right\} \\
 &= \mathcal{P}\left\{\frac{\cos \phi - \frac{t}{\tau}}{\sin \phi} \leq \frac{\sin \theta}{1 - \cos \theta} \leq \frac{\cos \phi + \frac{t}{\tau}}{\sin \phi}\right\}
 \end{aligned} \tag{16}$$

We define the random variable

$$X = \frac{\sin \theta}{1 - \cos \theta} \tag{17}$$

Given that $f_\theta(\theta) = \frac{1}{2\pi}$, $0 \leq \theta < 2\pi$, the CDF of X can be computed as follows:

$$\begin{aligned}
 F_X(x) &= \mathcal{P}\{X \leq x\} \\
 &= \mathcal{P}\left\{\frac{\sin \theta}{1 - \cos \theta} \leq x\right\} \\
 &= \mathcal{P}\left\{\sin \theta + x \cos \theta \leq x\right\} \\
 &= \mathcal{P}\left\{\Re\{(x - j)e^{j\theta}\} \leq x\right\} \\
 &= \mathcal{P}\left\{\sqrt{1 + x^2} \cos\left(\theta - \cos^{-1} \frac{x}{\sqrt{1 + x^2}}\right) \leq x\right\} \\
 &= \mathcal{P}\left\{\cos\left(\theta - \cos^{-1} \frac{x}{\sqrt{1 + x^2}}\right) \leq \frac{x}{\sqrt{1 + x^2}}\right\} \\
 &= \mathcal{P}\left\{2 \cos^{-1} \frac{x}{\sqrt{1 + x^2}} \leq \theta \leq 2\pi\right\} \\
 &= \int_{2 \cos^{-1} \frac{x}{\sqrt{1 + x^2}}}^{2\pi} \frac{1}{2\pi} d\theta \\
 &= 1 - \frac{1}{\pi} \cos^{-1} \frac{x}{\sqrt{1 + x^2}}
 \end{aligned} \tag{18}$$

We can now use (18) in (16) to obtain

$$\begin{aligned}
F_T(t|\phi) &= F_X\left(\frac{\cos\phi + \frac{t}{\tau}}{\sin\phi}\right) - F_X\left(\frac{\cos\phi - \frac{t}{\tau}}{\sin\phi}\right) \\
&= \frac{1}{\pi} \left(\cos^{-1} \frac{\cos\phi - \frac{t}{\tau}}{\sqrt{1 + (\frac{t}{\tau})^2 - 2(\frac{t}{\tau})\cos\phi}} - \right. \\
&\quad \left. - \cos^{-1} \frac{\cos\phi + \frac{t}{\tau}}{\sqrt{1 + (\frac{t}{\tau})^2 + 2(\frac{t}{\tau})\cos\phi}} \right) \quad (19)
\end{aligned}$$

The conditional PDF of T can be obtained by applying differentiation to (19), yielding

$$f_T(t|\phi) = \frac{1}{\pi\tau} \frac{2(1 + (\frac{t}{\tau})^2) \sin\phi}{1 + 2(\frac{t}{\tau})^2 + (\frac{t}{\tau})^4 - 4(\frac{t}{\tau})^2 \cos^2\phi} \quad (20)$$

The primitive of (20) with respect to ϕ is given by

$$\int f_T(t|\phi) d\phi = -\frac{1}{\pi t} \tanh^{-1} \left(\frac{2\frac{t}{\tau}}{1 + (\frac{t}{\tau})^2} \cos\phi \right) \quad (21)$$

Finally, we use (21) to compute the unconditional PDF of T , resulting in

$$\begin{aligned}
f_T(t) &= \frac{1}{\pi} \int_0^\pi f_T(t|\phi) d\phi \\
&= \frac{2}{\pi^2 t} \tanh^{-1} \frac{2\frac{t}{\tau}}{1 + (\frac{t}{\tau})^2} \quad (22)
\end{aligned}$$

References

- [1] M. Schnell and S. Scalise, *NEWSKY - NEtWorking the SKY Concept for Civil Aviation*, IEEE Aerospace and Electronic Systems Magazine, 22 (5), IEEE, ISSN 0885-8985, 2007.
- [2] D. Medina, S. Ayaz and F. Hoffmann, *Feasibility of an Aeronautical Mobile Ad Hoc Network Over the North Atlantic Corridor*, Fifth Annual IEEE Communications Society Conference on Sensor, Mesh and Ad Hoc Communications and Networks - SECON 2008, San Francisco, CA, June 2008.
- [3] IATA (International Air Transport Association) Schedule Reference Service (SRS), <http://www.iata.org/ps/publications/srs/>
- [4] E. Sakhaee and A. Jamalipour, *The Global In-Flight Internet*, IEEE Journal on Selected Areas in Communications, September 2006.
- [5] E. Sakhaee, A. Jamalipour and N. Kato, *Aeronautical Ad Hoc Networks*, IEEE Wireless Communications and Networking Conference (WCNC 2006).
- [6] M. Iordanakis *et al.*, *Ad-hoc Routing Protocol for Aeronautical Mobile Ad-Hoc Networks*, Fifth International Symposium on Communication Systems, Networks and Digital Signal Processing (CSNDSP), July 2006.
- [7] AeroSat Corporation, <http://www.aerosat.com>
- [8] Airborne Internet Consortium (AIC), <http://www.airborneinternet.org>
- [9] W. McNary, *Transformational Aircraft Communication Using a Broadband Mesh Network*, 7th ICNS Conference, May 2007, http://spacecom.grc.nasa.gov/icnsconf/docs/2007/Session_B/05-McNary.pdf
- [10] S. Ruffino and P. Stupar, *Automatic configuration of IPv6 addresses for MANET with multiple gateways (AMG)*, draft-ruffino-manet-autoconf-multigw-03, June 2006.
- [11] Y. Kim *et al.*, *Load-Balancing Proactive Internet Gateway Selection in MANET*, draft-kim-autoconf-gatewaysel-01, February 2007.
- [12] R. Wakikawa *et al.*, *Global connectivity for IPv6 Mobile Ad Hoc Networks*, draft-wakikawa-manet-globalv6-05, March 2006.
- [13] B. Karp and H. T. Kung, *GPSR: Greedy Perimeter Stateless Routing for Wireless Networks*. In *Proceedings of the Sixth Annual ACM/IEEE International Conference on Mobile Computing and Networking (MobiCom 2000)*.
- [14] J. Li *et al.*, *A Scalable Location Service for Geographic Ad Hoc Routing*. In *Proceedings of the Sixth Annual ACM/IEEE International Conference on Mobile Computing and Networking (MobiCom 2000)*.
- [15] H. Fuessler *et al.*, *A Comparison of Routing Strategies for Vehicular Ad-Hoc Networks*, Department of Computer Science, University of Mannheim, July 2002.
- [16] A. Festag, R. Baldessari and H. Wang, *On Power-Aware Greedy Forwarding in Highway Scenarios*, 5th International Workshop on Intelligent Transportation (WIT), Hamburg, Germany, March 2007.
- [17] Shephard Inflight Online, *Revolutionary broadband scheme looks to cut out satellite middlemen*, December 2005.